

Artificial trapping of a stable high-density dipolar exciton fluid

Gang Chen, Ronen Rapaport, L. N. Pfeifer, K. West, P.

M. Platzman, Steven Simon¹ and Z. Vörös, and D. Snoke²

¹*Bell Laboratories, Lucent Technologies,*

600 Mountain Avenue, Murray Hill, New Jersey 07974

²*Department of Physics and Astronomy,*

University of Pittsburgh, Pittsburgh, Pennsylvania 15260, USA

Abstract

We present compelling experimental evidence for a successful electrostatic trapping of two-dimensional dipolar excitons that results in stable formation of a well confined, high-density and spatially uniform dipolar exciton fluid. We show that, for at least half a microsecond, the exciton fluid sustains a density higher than the critical density for degeneracy if the exciton fluid temperature reaches the lattice temperature within that time. This method should allow for the study of strongly interacting bosons in two dimensions at low temperatures, and possibly lead towards the observation of quantum phase transitions of 2D interacting excitons, such as superfluidity and crystallization.

The different thermodynamic phases of a system of particles and the transitions between them is fundamental to our understanding of the material world. Most notably, the dimensionality of the particle system, together with the importance of quantum statistical effects, can have a profound impact on its physical behavior. Two-dimensional (2D) systems of interacting particles are expected to have a rich and unique behavior. They are, however, experimentally much more challenging to realize than their three dimensional counterparts, and 2D bosons, especially in solid state systems, are essentially unexplored experimentally.

One of the most promising 2D system of bosons is that of 2D excitons, which are coulomb bound electron-hole pairs confined in a semiconductor quantum well layers. In the dilute limit, where $n_X^{-1/2} \gg a_X$ (n_X being the exciton 2D density and a_X is the Bohr radius), excitons can be considered as bosons, as the identity of their fermionic constituents is essentially hidden within the excitonic atomic-like structure. It has been predicted that 2D excitons at low temperatures can undergo a quantum phase transition to either a Bose-Einstein condensate [1] similar to trapped alkali atoms [2], or to a condensed superfluid state [3, 4, 5], similar to, for instance, superfluid ^4He . A clear observation of this elusive phase remains one of the tough but most interesting challenge that low-dimensional systems physicists have been working toward for the past several decades [6, 7].

During the past decade, a unique class of 2D excitons, that are spatially indirect, has been introduced to this field of study. In these spatially indirect systems, the constituent electrons and holes are separated into two weakly coupled quantum wells with an inter-well energy barrier [8, 9]. This separation results in two unique features. First, the exciton lifetime can become extremely long (in the microseconds regime), a crucial requirement for thermalization processes [10, 11, 12]. Secondly, the indirect excitons are intrinsically dipolar, and their dipole moments are *all* aligned perpendicular to the quantum wells plane, resulting in a net dipole-dipole repulsive interaction between them. This short range interaction is expected to play a crucial role in the physics of quantum phase transitions of such an exciton fluid, which is a good model system for interacting bosons in two dimensions. However, as we have recently suggested, the exciton permanent dipole moment also prevents the optically excited dipolar excitons from forming a stable fluid and from maintaining densities high enough for a quantum phase transition to occur [12], as this exciton fluid tends to rapidly expand under its own repulsive forces [12, 13]. This expansion can prevent other possible interesting phases such as exciton crystallization [14], which requires a stable and

well confined fluid.

It is tempting to try and exploit several of the concepts that were so successful in atomic physics in order to overcome the expansion problem and achieve a high-density, stable and long-lived exciton gas. We have recently proposed a scheme for trapping a high-density exciton fluid in a quantum well plane [15, 16]. This scheme utilizes the interaction of the exciton dipoles with an externally applied local electric field to create an effective barrier that prevents the exciton fluid from expanding. In this report, we present compelling evidence for the successful implementation of our scheme, and show that in the presence of such a dipolar exciton trap, a high-density, stable, and spatially uniform exciton fluid is maintained in a confined and controlled configuration. We show that, for at least half a microsecond, the exciton fluid sustains a density higher than the critical density for degeneracy if the exciton fluid temperature reaches the lattice temperature within that time. We believe this demonstration is a major step towards the observation of quantum phase transitions of 2D interacting excitons and the possible exciton crystallization.

We follow our exciton trap (Xtrap) concept and design developed in Ref. 15, where dipolar excitons are trapped under local electrostatic gates. GaAs/AlGaAs double quantum well (DQW) structures are grown on top of an n^+ doped GaAs substrate [17]. Circular semi-transparent Ti gates (20nm thick, see Fig. 1b) with different diameters ($D = 4 - 80\mu\text{m}$) are deposited on top of the DQW samples. An electric bias (typically few volts) is applied to each of the gates via a narrow Ti evaporated wire (1-2 μm wide). The conductive substrate is used as the bottom electrode. This configuration is illustrated in Fig. 1a. The sample thickness between the two electrodes is l , while the DQW structure is grown at a distance z as measured from the bottom electrode. Two samples are described here. Both have a similar DQW structure and similar gate designs, and the main difference between them is their z/l ratio. One (sample A) has $z/l \simeq 0.03$ while the other (sample B) has $z/l \simeq 0.3$.

The dipolar exciton trapping takes place due to their interaction with the applied electric field under the biased Xtrap gate: dipolar excitons (with a dipole moment $\vec{d}_X = -ez_0\hat{z}$ [17]), are "high field seekers", i.e., when they are aligned parallel to an electric field \vec{E} , they will always seek its maximum, as their total energy is reduced by the dipole-field interaction term: $\varepsilon_{df} = \vec{d}_X \cdot \vec{E}(r_{\parallel}, z) = d_X E_z(r_{\parallel}, z)$. Thus applying an external bias locally to the gate results in an effective confining potential for the dipolar excitons under the gate [15]. An alternative way of understanding the trapping mechanism is to note that, as is shown in

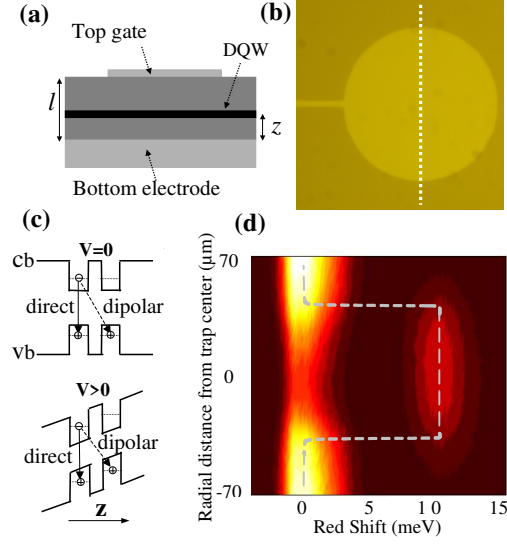


FIG. 1: (Color online)(a) A schematic of the Xtrap configuration. (b) A microscope image of an Xtrap upper gate with a diameter $D = 50\mu\text{m}$. The wire is $2\mu\text{m}$ wide. (c) The DQW band diagram under the top gate in the absence (upper) and the presence (lower) of an applied gate bias. Outside the gate, the band is flat, regardless of the bias. The two arrows represent the direct and indirect exciton transitions. (d) Spatially resolved PL spectra from an $80\mu\text{m}$ Xtrap (sample A) collected from a radial cross-section of the top gate (along the white dotted line in (b)), with a defocused He-Ne excitation and a bias of 3V. The dashed white line is the calculated electrostatic potential. The energy axis shows the red shift of the emission from the direct exciton emission line whose actual position is at 1.5567 eV (797 nm).

Fig. 1c, the applied electric field under the gate tilts the band structure in the \hat{z} direction, hence lowering the dipolar exciton transition energy locally. To experimentally measure the Xtrap energy profile, we spatially resolve the photoluminescence (PL) emission energy of the dipolar excitons, by collecting emission spectra along a radial cross-section of the Xtrap. An example of such spectral image is shown in Fig. 1d, taken from a $80\mu\text{m}$ diameter Xtrap of sample A at $T=5\text{K}$ with an applied bias of 3V, excited using a defocused cw He-Ne laser at 632.8nm and collected with a liquid nitrogen cooled CCD camera mounted at the exit port of a spectrometer. The confining potential profile can be clearly seen from the red-shifted PL under the gate. The emission energy outside the trap corresponds to zero field, or "direct" exciton line at 1.5567eV. The white dashed line is the calculated Xtrap potential

(see Ref. [15]), which nicely fits the experimental data.

Ideally, for diameter $D \gg l$, such an Xtrap confines a circular "pool" of dipolar excitons which are free-moving under the trap gate and experience a strong reflecting force near its boundary. While this seems simple enough, we have shown before that any in-plane fields at the Xtrap boundary, arising from the above gate geometry, can cause rapid ionization of excitons through field-induced tunneling, thus significantly degrading the Xtrap quality and making it very leaky [15]. Such a loss of excitons can be represented by an effective Xtrap lifetime, that can be orders of magnitude shorter than the intrinsic lifetime of the dipolar excitons, making the trapping very inefficient. A possible suggested solution [15, 18], is to design an Xtrap with the DQW structure grown very close to the conductive substrate (corresponding to a small z/l ratio), where the in-plane components of the electric field rapidly vanish. Since the ionization rate depends exponentially on the magnitude of the in-plane field component, a small z/l is expected to be a very important requirement for a high quality Xtrap, which is crucial for achieving a high-density, spatially uniform, and long-lived exciton fluid. In what follows we will present evidence that indeed, with the right design, such a high quality Xtrap is feasible.

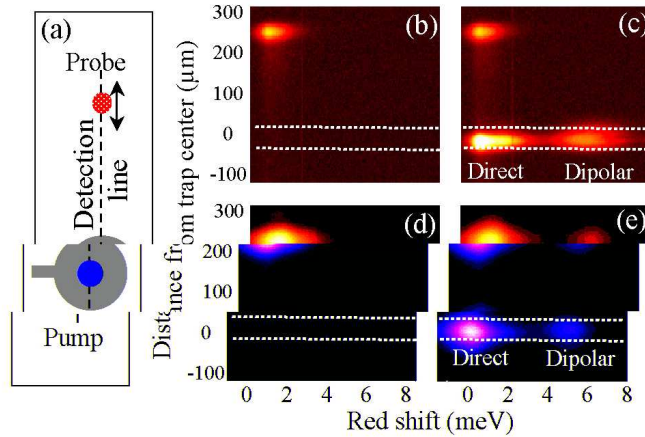


FIG. 2: (Color online)(a) Geometry of the PL pump-probe experiment on an $50\mu\text{m}$ diameter Xtrap. The PL is spatially resolved along the dashed line with its energy shown as a red shift from the direct exciton line. PL spectral images from sample A with (b) pump off, and (c) pump on. The pump power is $30\mu\text{W}$ and dipolar exciton red shift is 5 meV. PL spectra for sample B with (d) pump off, and (e) pump on taken under identical conditions. The white dotted lines mark the trap boundary.

To investigate the effect of the exciton ionization at the edge of the trap, we developed a spatially resolved "excitation pump-probe" technique: an "excitation-pump" from a non-resonant, cw He-Ne laser ($\lambda = 632.8\text{nm}$), is focused to the center of an Xtrap ($r_{\parallel} = 0$). An additional, similar but weak "excitation-probe" beam is focused outside the trap where no external bias was applied. The experimental geometry is shown in Fig. 2a. The PL of excitons created locally by this second beam was monitored, and the details of this local PL spectrum are directly related to the local environment of the probing excitons. If there is a significant ionization of dipolar excitons that are created by the excitation-pump within the Xtrap, the probing excitons created by the weak excitation outside the trap will interact with the ionized carriers leaking from the Xtrap and their emission will be spectrally modified. Fig. 2 presents the spatially resolved PL spectra along a line going through an $50\mu\text{m}$ diameter Xtrap center for the two samples A and B. The PL energy is measured as a red shift from the direct exciton transition energy. Fig. 2b-c show the such PL spectra from sample A ($z/l = 0.03$) with the excitation-pump (inside the Xtrap) off and on respectively. For the *entire* range of pump excitation powers and gate bias, we find that the probe PL is independent of the presence of the excitation-pump at the center of the trap, even for excitation-probe positions that are very close to the trap boundary (not shown). The probe excitons PL always corresponds to the transition energy and lineshape of direct excitons, consistent with the zero bias conditions expected outside of the Xtrap and is an indication of the high quality of the trap boundaries in sample A. On the contrary, the probe PL behavior of sample B ($z/l = 0.3$) is remarkably different: With pump-excitation off, the PL of the probe excitons is similar to that observed in sample A, as is shown in Fig. 2d. However, as the pump-excitation beam is turned on, these PL spectra are dramatically modified, and we observe an additional probe PL peak at the lower energy side of the direct exciton emission line, as is shown in Fig. 2e. This dramatic change of the remote probe PL can only be explained by a *leakage of carriers* from the Xtrap to the location of the probe, changing the local electrostatic environment and thus affecting the emission.

To understand the dynamics of the trapped excitons and verify the trap quality we measured the time dependence of the spatial cross-sectional profile of the PL from an $80\mu\text{m}$ diameter Xtrap (6V , $\sim 30\text{meV}$ deep) of sample A, after a short pulse excitation (pulse width 2ps , repetition rate 250 KHz , spatial $\text{FWHM} \simeq 40\mu\text{m}$, and excitation intensity $200\text{ }\mu\text{W}$), resonant with the direct exciton transition. The dipolar exciton density immediately after

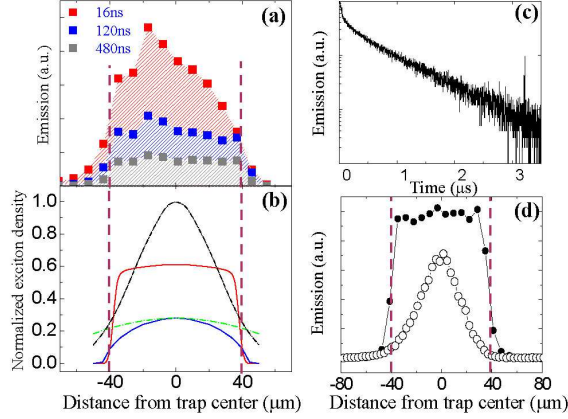


FIG. 3: (Color online)(a) Spectrally integrated intensity of the dipolar exciton PL along a radial cross-section of an 80μm Xtrap of sample A with a potential depth of 30meV, for three different times after the initial excitation ($\text{FWHM} \simeq 30\mu\text{m}$). (b) Calculated exciton density 120ns after excitation for the case of reflecting Xtrap boundaries (solid-red), absorbing Strap boundaries (solid-blue), and no boundaries (dash-dot green). The black dash-dotted curve presents the initial exciton distribution. (c) The time trace of the spectrally integrated PL at the center of the trap in (a). (d) Time integrated spatial profile of dipolar excitons from an 80 μm trap of sample A (black dots) and B (open circles) excited by 10 ns pulses with $\text{FWHM} \simeq 40\mu\text{m}$. The dashed lines mark the position of the trap.

the laser excitation pulse is estimated to be $\sim 8 \times 10^{10} \text{cm}^2$ (based on a method to be discussed later). The PL was spectrally integrated over the whole dipolar exciton spectral line and detected using a single photon counting photomultiplier tube. The details of this measurement technique is given in Ref. 13. PL profiles at several times after the optical excitation are shown in Fig. 3a. The boundary of the trap is marked by the dashed lines. Shortly after the excitation, the PL profile is nearly Gaussian, already broader but similar in shape to that of the excitation beam. The PL profile continues to rapidly expand toward the trap edges and to flatten. After $\sim 100\text{ns}$ the PL profile becomes completely flat with a sharp drop at the trap boundaries, only limited by the imaging resolution, and decays uniformly with time (the small and sharp peak at $\sim 20\mu\text{m}$ is due to scattering of residual laser pulses). A time trace of the PL at the center of the trap is plotted in the Fig. 3c, showing the exponential decay with a microsecond time constant after the profile has flattened (the

initial faster decay is mainly due to the expansion of the exciton fluid within the trap). Such a behavior is indeed expected from a combination of an outward expansion driven by the effective net dipolar repulsion force and the sharp profile of reflecting forces *with negligible losses* at the Xtrap boundary. The above measurements are consistent with a calculation of the expansion dynamics in the Xtrap, based on the model we developed in Ref. [12] for free expansion of dipolar excitons, but with the addition of an external electrostatic trap potential barrier[19]. The calculated exciton profile 120 ns after the excitation, shown by the red curve in Fig. 3b, nicely reproduces the expansion and flattening of the exciton distribution. In contrast, the calculated exciton profile for absorbing trap boundaries (as is expected if a fast exciton ionization takes place) and that of expanding excitons with no boundaries, shown by the blue and green curves respectively, always keep their curvature and do not show flattening at any stage of the expansion. This is verified by Fig. 3d which shows a comparison between the time integrated spatial emission profile from an 80 μm trap of sample A (black dots) and B (open circles). In addition, the fact that the decay time of the excitons is similar to their intrinsic lifetime is a strong evidence that exciton loss at the Xtrap boundary is insignificant. All of the above findings therefore confirm high quality Xtraps in sample A, with good reflecting boundaries and negligible ionization.

For a lattice temperature of 1.4K of the experiment in Fig. 3, the critical density for degeneracy is $\simeq 2 \times 10^{10} \text{cm}^{-2}$. Fig. 3c shows that for at least half a microsecond the exciton fluid sustains a density higher than that critical density. The exciton fluid is highly degenerate if it is thermalized with the lattice within that time.

To show the dramatic effect of the exciton trapping, we now compare free expanding dipolar excitons to trapped ones. When the bias is applied uniformly to the whole sample (via a very large gate, millimeters in size), the dipolar excitons that are optically excited at a small spot diameter ($\sim 30 \mu\text{m}$) expand as a result of dipolar repulsion due to the radial density gradient. For a dipolar exciton lifetime that exceeds 1 μs , the exciton fluid can rapidly expand to hundreds of microns in diameter [12, 13]. This is shown in the image of Fig. 4a, which was taken by spectrally resolving the emission from a slice passing through the excitation spot created using a cw He-Ne laser. Here, the vertical axis shows the spatial expansion of the dipolar exciton fluid and the horizontal axis represents the PL energy, measured as red shift relative to the direct exciton transition energy. As expected, at the center of the excitation spot, the steady state density of dipolar excitons is higher, thus the

applied bias is partially screened, leading to a slightly blue shifted emission compared with positions further away from the excitation spot, where the exciton density decreases and thus the emission corresponds to that of dilute dipolar excitons. In contrast, the PL coming from a $50\mu\text{m}$ diameter Xtrap, *under the same excitation conditions* is very different, as is shown in Fig. 4b. It clearly shows no PL outside the trap, and a larger blue shift (compared to the free excitons), indicating higher exciton density.

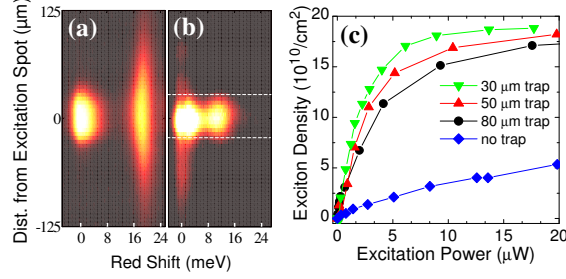


FIG. 4: (Color online)(a) Spatially resolved PL spectra of (a) free expanding dipolar excitons, (b) dipolar excitons confined in a $D = 50\mu\text{m}$ trap, with a cw He-Ne laser excitation. The emission lines at a zero red shift are due to the direction exciton emission. The bias is 4V and the excitation power is $30\mu\text{W}$. The dashed lines mark the trap boundaries. (c) The extracted dipolar exciton density at the center of the excitation spot as a function of the cw laser excitation power on the sample surface for free expanding and trapped excitons. The applied bias is 6V.

Neglecting small corrections from dipole-dipole interaction, the dipolar exciton PL energy blue shift (compared to the dilute case) is proportional to the fluid density due to the density dependent screening of the external applied field by the dipoles [12, 15]. This dependence can be written as: $\Delta\varepsilon = (4\pi e^2 z_0 / \epsilon) n_X$, where n_X is the local exciton density and ϵ is the background dielectric constant. This allows for an approximate calibration of the experimental dipolar exciton density. In Fig. 4c, we present the steady-state exciton density as a function of the excitation power at the sample surface for various gate sizes, under the same experimental conditions. The dipolar exciton density is thus obtained by monitoring the blue shift, $\Delta\varepsilon$, of the emission from the center of the PL profile as the excitation intensity increases. Fig. 4c shows that due to the driven expansion induced by the dipolar repulsion, the achievable density of free dipolar excitons (with no trap) is always far below that can be obtained in the Xtraps. At high excitation intensities, exciton densities as

high as $1.8 \times 10^{11} \text{cm}^{-2}$ are observed in Xtraps, approaching the limit where the inter-exciton spacing becomes comparable to the exciton Bohr radius. The increase of exciton density in Xtraps becomes sublinear at high excitation intensities. The mechanism for this sublinear behavior seems to be a partial filling of the trap as the power is increased, and consequently an expected decrease in the exciton lifetime [9] ($n_X = G\tau_X(G)$, where G is the exciton photogeneration rate and τ_X is the filling dependent and hence the power dependent exciton lifetime). With the same excitation powers, a larger steady exciton density is observed in the smaller Xtraps, as optically excited excitons spread over a smaller trap area. It is then clear that by making a high quality exciton trap, one can indeed achieve a confined, high-density, long-lived, and homogeneously distributed exciton fluid.

We now briefly discuss the expected unique physical properties of the dipolar exciton gas that is confined in the Xtrap. The De-Broglie temperature, which mark the approximate transition to the regime where quantum statistics starts to play an important role, is $T_{Xqs} \simeq 0.7(n_X/10^{10})K$ (where n_X is in units of cm^{-2}). On the other hand, the classical nearest-neighbor dipole-dipole interaction term, calculated for a square dipolar exciton lattice in equilibrium is $\varepsilon_{dd}^{eq}/k_B = (4d_X^2/(k_B\epsilon))n_X^{3/2} \simeq 1.3(n_X/10^{10})^{3/2}K$, and the harmonic potential for small vibrations is approximated to be $\hbar\omega_X/k_B = \sqrt{18\hbar^2d_X^2/(k_B^2\epsilon m_X)}n_X^{5/4} \simeq 1.57(n_X/10^{10})^{5/4}K$ [20]. As one can see, it turns out that at the relevant experimental densities in the Xtrap ($n_X \sim 10^{10}\text{cm}^{-2}$), all these physical quantities are of the same order of magnitude, which can lead to some very interesting consequences in terms of the possible thermodynamic phases of the excitons, such as a possible competition of the quantum superfluid phase with the exciton crystal phase. Note that crystallization of particles with a net repulsive interaction can only happen within a confined volume and thus is expected to be unique to the dipolar excitons in the trap. What happens to a 2D dipolar exciton fluid in this regime is yet to be explored.

-
- [1] L. V. Keldysh and A. N. Kozlov, JETP **27**, 521 (1968).
 - [2] J. R. Anglin and W. Ketterle, Nature **416**, 211 (2002).
 - [3] J. M. Kosterlitz and D. J. Thouless J. Phys. C **6**, 1181 (1973).
 - [4] Y. E. Lozovik and V. I. Yudson, JETP lett. **22**, 274 (1975), and S. I. Shevchenko, Sov. J. Low

- Temp. Phys. **2**, 251 (1976).
- [5] J. Fernandez-Rossier, C. Tejedor, Phys. Rev. Lett. **78**, 4809 (1997).
 - [6] For reviews see: D. Snoke, Science **298**, 1368 (2002) and L. V. Butov, J. Phys.: Condens. Matter. **16** R1577 (2004).
 - [7] J. P. Eisenstein and A. H. MacDonald, Nature **432**, 691 (2004).Rev. Lett. **78**, 4809 (1997).
 - [8] T. Fukuzawa, E. E. Mendez, and J. M. Hong, Phys. Rev. Lett. **64**, 3066 (1990).
 - [9] A. Alexandrou, J. A. Kash, E. E. Mendez, M. Zachau, J. M. Hong, T. Fukuzawa, and Y. Hase, Phys. Rev. B **42** 9225 (1990).
 - [10] R. Rapaport, Gang Chen, D. Snoke, Steven H. Simon, Loren Pfeiffer, Ken West, Y. Liu, and S. Denev, Phys. Rev. Lett. **92**, 117405 (2004).
 - [11] L. V. Butov, L. S. Levitov, A. V. Mintsev, B. D. Simons, A. C. Gossard, and D. S. Chemla, Phys. Rev. Lett. **92**, 117404 (2004).
 - [12] R. Rapaport, G. Chen, and S. Simon, Phys. Rev. B **73**, 033319 (2006).
 - [13] Z. Vörös, R. Balili, D.W. Snoke, L. N. Pfeiffer, and K. West, Phys. Rev. Lett. **94**, 226401 (2005).
 - [14] G. Schmid, S. Todo, M. Troyer, and A. Dorneich, Phys. Rev. Lett. **88**, 167208 (2002).
 - [15] R. Rapaport, Gang Chen, Steven H. Simon, Oleg Mitrofanov, Loren Pfeiffer, and P. M. Platzman, Phys. Rev. B **72**, 075428 (2005).
 - [16] For previous work on confining excitons in single quantum well structures under interdigitated gates, see S. Zimmermann, G. Schedelbeck, A. O. Govorov, A. Wixforth, J. P. Kotthaus, M. Bichler, W. Wegscheider, and G. Abstreiter, Appl. Phys. Lett. **73**, 154 (1998) and the refereces therein.
 - [17] The two samples consist of a DQW structure grown on an n^+ doped GaAs substrate. The two GaAs QWs are 100\AA wide separated by a 40\AA $\text{Al}_{0.45}\text{Ga}_{0.55}\text{As}$ barrier and are cladded by 500\AA $\text{Al}_{0.45}\text{Ga}_{0.55}\text{As}$ barriers. The nominal separation between the two QW centers is $z_0 = 140\text{\AA}$. In the absence of external bias, the direct exciton transition is at 1.5567 eV (797 nm). The indirect dipolar exciton transition energies qouted in this paper are relative to the above value.
 - [18] A. T. Hammack, N. A. Gippius, G. O. Andreev, L. V. Butov, M. Hanson, and A. C. Gossard, Condmat/0504045 (2005).
 - [19] R. Rapaport, Unpublished (2005).
 - [20] We use the following parameter values: $m_X = 0.2m_e$, $\epsilon = 10$ and $z_0 = 14nm$.